



EUROPEAN SOUTHERN OBSERVATORY
OBSERVATOIRE DE GENÈVE
OBSERVATOIRE DE HAUTE-PROVENCE
UNIVERSITÄT BERN
SERVICE D'AÉRONOMIE

OBSERVATOIRE DE HAUTE-PROVENCE

F-04870 ST.MICHEL L'OBSERVATOIRE - FRANCE
PHONE: +33 (0) 492 70 64 00 - FAX: +33 (0) 492 70 64 64

HARPS

Optics Final Design Report

Doc. No. 3M6-TRE-HAR-33103-0004

Issue 2.0

February 28, 2000

Prepared Dominique Kohler.....28/02/2001.....
Name Date Signature

Approved Francesco Pepe.....28/02/2001.....
Name Date Signature

Released Michel Mayor.....28/02/2001.....
Name Date Signature

Change Record

Issue/Rev.	Date	Section/Page affected	Reason/Remarks
1.0	March 13, 2000	All	First issue for FDR Optics
1.1	June 26, 2000	Document number All Introduction Compliance Matrix	Changed Updated for HARPS PDR New New
2.0	February 28, 2001	Camera Optics Collimator F/N-conversion optics All	New glasses Focal length changed Added/Updated Updated for FDR

Table of Contents

CHAPTER 1: INTRODUCTION	5
1.1 SCOPE AND FOREWORD.....	5
1.2 DOCUMENTS.....	5
1.2.1 <i>Applicable Document</i>	5
1.2.2 <i>Reference Document</i>	5
1.3 ACRONYMS	6
1.4 CONTRIBUTIONS TO THIS DOCUMENT	6
CHAPTER 2: GENERAL DESCRIPTION	7
CHAPTER 3: OPTICAL COMPONENTS	9
3.1 FIBERS AND F/N ADAPTATION OPTICS	9
3.2 COLLIMATORS	10
3.3 FLAT FOLDING MIRROR.....	11
3.4 ECHELLE GRATING.....	12
3.5 CROSS-DISPERSER GRISM	13
3.5.1 <i>General Considerations</i>	13
3.5.2 <i>Transmission Efficiency</i>	13
3.5.3 <i>Operating Conditions</i>	14
3.5.4 <i>Characteristics of the Cross-Disperser Grism</i>	14
3.6 CAMERA OPTICS	15
3.6.1 <i>Description of the Camera Optics</i>	15
3.6.2 <i>Optical Characteristics</i>	16
3.6.3 <i>Camera Optics Efficiency</i>	18
3.6.4 <i>Order-Separating Filter</i>	18
CHAPTER 4: SPECTROGRAPH PERFORMANCES	19
4.1 SPECTRAL FORMAT	19
4.2 SPOT DIAGRAMS AND IMAGE QUALITY	20
4.3 OPTICAL EFFICIENCY.....	23
4.3.1 <i>Mirror Coating</i>	23
4.3.2 <i>Lens AR Coating</i>	23
4.3.3 <i>Overall Efficiency</i>	23
4.3.4 <i>Vignetting</i>	23
4.4 GHOST IMAGES AND PARASITIC LIGHT	24
4.4.1 <i>Camera Optics Ghost Analysis</i>	24
4.4.2 <i>Ghosts from the Grism</i>	26
4.4.3 <i>Echelle Grating Ghosts</i>	27
4.4.4 <i>Conclusions</i>	27
4.5 ENVIRONMENTAL SENSITIVITY	28
4.5.1 <i>Thermal Influence</i>	28
4.5.2 <i>Effects of Air Pressure</i>	29
CHAPTER 5: ALIGNMENT AND TOLERANCES	30
5.1 BASIC OPTO-MECHANICAL PRINCIPLES	30
5.2 MAIN ALIGNMENT CONTROLS	30
5.3 ALIGNMENT TOOLS	30
5.4 ALIGNMENT TOLERANCES	31
CHAPTER 6: COMPLIANCE MATRIX	32
CHAPTER 7: APPENDIX	35

7.1	SPECTROGRAPH LENS DATA	35
7.2	F/N-CONVERSION OPTICS LENS DATA	38

List of Tables

Table 1:	General parameters of the HARPS spectrograph	8
Table 2:	Characteristics of the collimator parabola	11
Table 3:	Characteristics of the echelle grating	12
Table 4:	Calculated grism efficiency for the parameters shown in Table 5	13
Table 5:	Characteristics of the grism	15
Table 6:	Lens data of the camera optics.....	16
Table 7:	Characteristics of the camera optics	17
Table 9:	Geometrical characteristics of the echelle orders	20
Table 10:	Spectrograph efficiency.....	23
Table 12:	Vignetting through the entire spectrograph.	24
Table 13:	Stability of HARPS (non compensated)	28
Table 14:	Stability of HARPS(<i>compensated</i>)	29
Table 15:	Changes in focal length in vacuum.....	29

List of Figures

Figure 1:	Ray tracing of the HARPS spectrograph.....	7
Figure 2:	Raytracing of the F/N adaptation optics.....	9
Figure 3:	Spot diagram of the F/N adaptations optics	10
Figure 4:	Collimator parabola. The gray zones indicate the used areas.	11
Figure 5:	Flat folding mirror	12
Figure 6:	Operating condition of the cross-disperser grism.....	14
Figure 7:	Ray tracing of the camera optics	16
Figure 8:	Spot diagrams of the camera optics only.....	17
Figure 10:	Field lens and order-separating filter.....	18
Figure 12:	Spectral format. The gray rectangles represent a mosaic of two 2k4 CCDs.	19
Figure 13:	Spot diagrams of the HARPS spectrograph.....	21
Figure 14:	Numbering of the lens surfaces	25

Chapter 1: Introduction

1.1 Scope and Foreword

This document describes in detail the optical characteristics and performances of the HARPS spectrograph optics. It intends to demonstrate that HARPS will meet the specified performances. This document, reviewed at Optics FDR in April 2000, has been updated for PDR held in June 2000. After ordering the camera optics, one of the employed glasses turned out not to be deliverable. The camera optics design had to be modified slightly. During the final definition of the optical design also two additional parameters have been modified: The first change concerns the focal length of the collimator which has been increased from 1500 mm to 1560 mm. The theoretical entrance pupil has consequently changed from 200 mm to 208 mm. The second change concerns two of the camera optics lenses. For them SFPL51 has been used instead of SFPL51Y. This document is the updated FDR document in which these modifications have been considered.

1.2 Documents

1.2.1 Applicable Document

AD-1	HARPS Technical Requirements Specifications	3M6-SPE-HAR-33100-0002	1.0	21/06/2000
------	---	------------------------	-----	------------

1.2.2 Reference Document

RD-1	HARPS Echelle Grating SOW and Requirements Specifications	3M6-SOW-HAR-33103-0001	1.0	8/2/2000
RD-2	Test results of 31.6 gr/mm R-4 red echelle grating	VLT-VER-ESO-132000-0850	1.0	26/05/1995
RD-3	HARPS Grism SOW and Requirements Specifications	3M6-SOW-HAR-33103-0002	1.2	12/02/2001
RD-4	HARPS Camera SOW and Requirements Specifications	3M6-SOW-HAR-33103-0003	1.0	11/05/2000
RD-5	Test Results of the 31.6 gr/mm R4 Red Echelle Mosaic	VLT-VER-ESO-13200-0850	1.0	26/05/1995
RD-6	Vacuum Vessel Temperature Control System	3M6-TRE-HAR-33102-0005	1.0	28/02/2001

1.3 Acronyms

AAA	Astronomical Absolute Accelerometer
AD	Applicable Document
AR	Anti-Reflection (coating)
CCD	Charge-Coupled Device
CFA	Cassegrain Fiber Adapter
FDR	Final Design Review
HARPS	High-Accuracy Radial-velocity Planetary Search (spectrograph)
HeNe	Helium-Neon (laser)
PDR	Preliminary Design Review
RD	Reference Document
UV	Ultra-Violet (light)
UVES	Ultra-violet-to-Visual Echelle Spectrograph

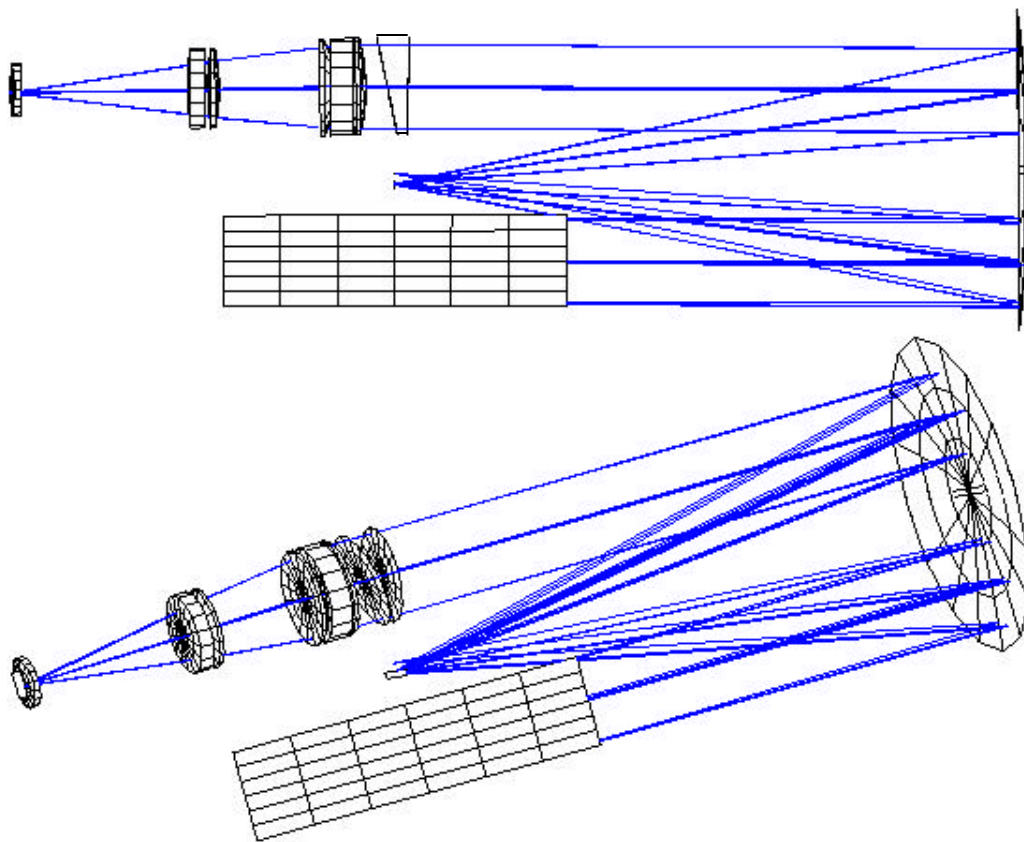
1.4 Contributions to this Document

François Bouchy	OG	Section Spectral Format
Bernard Delabre	ESO	Section Ghost Analysis

Chapter 2: General Description

HARPS is a fiber-fed, cross-dispersed echelle spectrograph. The optical design is similar to the concept of UVES. This is probably one of the best solutions for a cross-dispersed and very high-resolution spectrograph, which requires an R4 echelle grating. It uses an F/7.5 collimator, which allows a relatively compact spectrograph still being in accordance with the limiting F-number of the collimator in term of optical quality and manufacturing difficulties. A ray tracing of the complete HARPS spectrograph is shown in Figure 1. The full Zeemax report is enclosed in the Appendix.

Figure 1: Ray tracing of the HARPS spectrograph



Two optical fibers are required for the HARPS spectrograph to be used in simultaneous-thorium mode. Only one of them will be used in the iodine mode. The optical fibers feed the spectrograph with an F/4 beam, which is converted by small conversion optics into a F/7.5 beam to match the collimator-beam aperture. The collimator consists of a single parabolic mirror of 750 mm in diameter and with a focal length $f = 1560$ mm. It is employed off-axis and in triple pass. At the first pass the beam is collimated and sent to the R4 echelle grating operated in quasi-Littrow conditions with a small off-plane angle of $\epsilon = 0.721^\circ$. The dispersed beam is sent back to the parabola, which collects the beam to form at its focus an intermediate spectrum with spatially

superposed echelle orders. A flat folding mirror located at the position of the intermediate spectrum sends for a third pass the beam to the parabolic mirror in order to collimate it again for cross dispersion. The cross disperser is a grism. In order to minimize its clear diameter it is positioned at the image of the pupil defined by the echelle grating. The cross-disperser grism separates spatially the overlapping echelle orders. Finally, the beam is collected by the highly efficient camera optics ($F/3.3$, $f = 725$ mm). The object and the reference spectra are imaged on the CCD detector order by order. A summary of the HARPS optical performances is given in Table 1.

Table 1: General parameters of the HARPS spectrograph

# of fibers feeding the spectrograph	2
Accepted field by the fiber	1 arcsec
Collimated beam diameter	208 mm
Spectral range	380 nm - 690 nm
Image quality over spectral format area	< 2 pixels
Spectral resolution	$R \approx 84'000$
Spectral format (x,y)	62.74 mm x 61.44 mm
Photosensitive area	mosaic of two 2k x 4k CCDs
Pixel size	15 μm
Pixel sampling	4 pixels/SE
Distance between object and reference fiber projected on the CCD (center to center)	17 pixels

Chapter 3: Optical Components

3.1 Fibers and F/N Adaptation Optics

The spectrograph is fed by $70\ \mu\text{m}\varnothing$ fibers. The fibers exits will be mounted at the focus of the collimator parabola. Small F/N-adaptation optics converts the output F/4 beam to a F/7.5 beam to feed the collimator parabola. A first doublet, glued on the fibers to reduce exit losses, collimates the beam. A second doublet converts the beam in a F/7.5 beam. An intermediate image of the fiber exit is formed about 15 mm after the second doublet. This configuration has the advantage that a mask could be placed at this location to cut possible stray light. In addition, it allows installing the AAA displacement mechanism in future. A ray tracing of the F/N-adaptation optics is shown in Figure 2. Lens data are included in the Appendix of this document.

Figure 2: Raytracing of the F/N adaptation optics

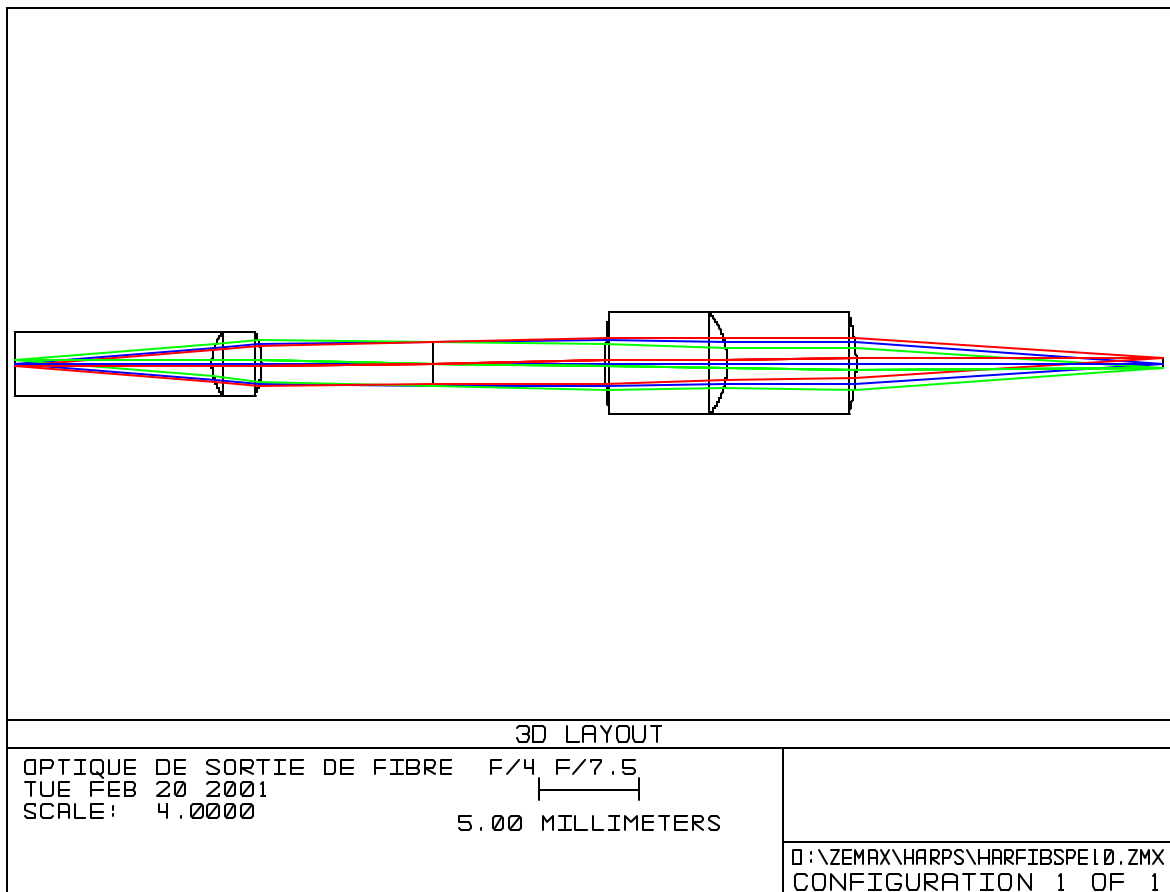
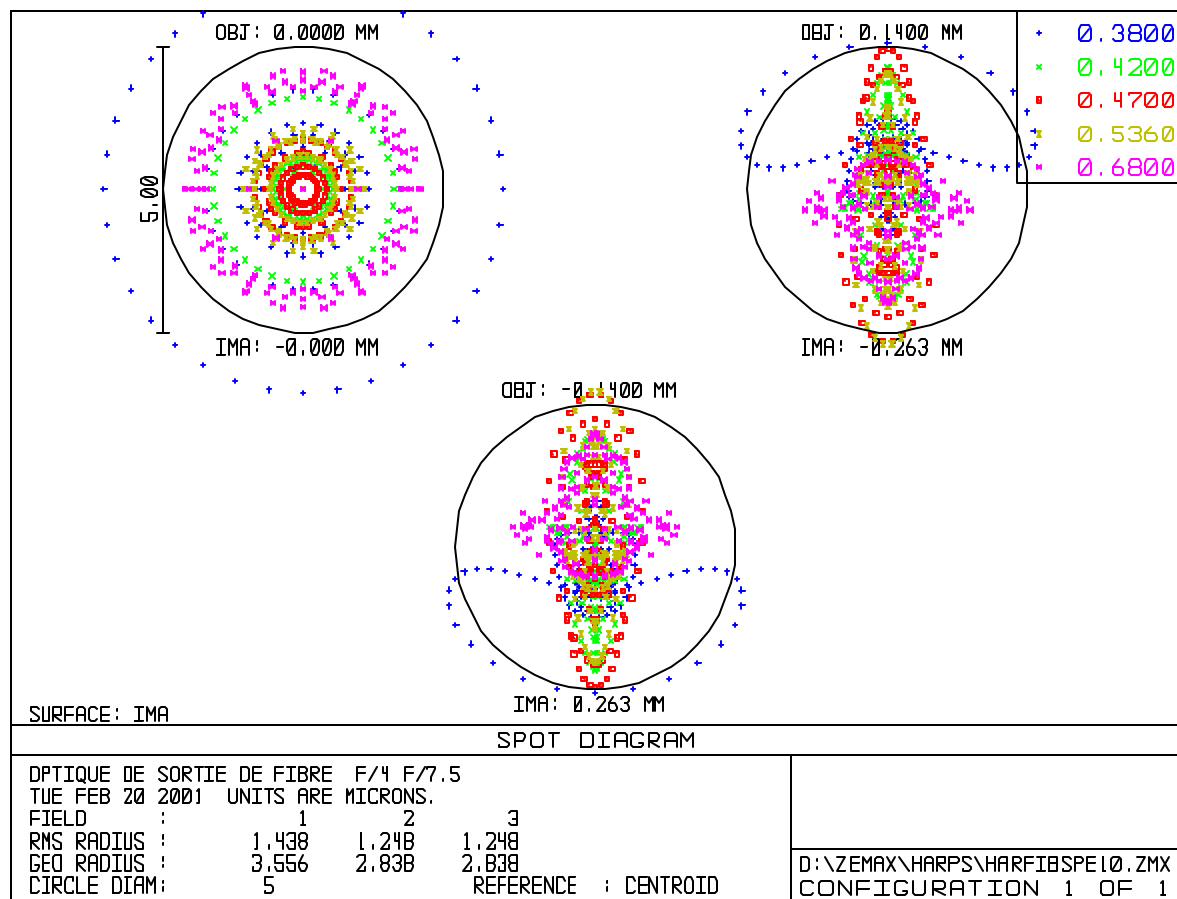


Figure 3 shows the spot diagrams of the F/N-conversion optics. The two off-axis object positions correspond to the position of the fiber exit of the object and reference fiber, respectively. The image quality has been optimized for these positions. The central position is only shown for completeness. The image quality is excellent. The circle indicates a diameter of 5 μm . This value has to be compared with the size of the fiber exit image, which is about 120 μm . Therefore, no degradation of the overall image quality of the spectrograph is expected to be produced by this system.

The optical efficiency is expected to be very good. High-transmittance glasses have been used. All surfaces are coated. Since the first doublet is glued on the fiber exit, the exit losses, which could attain up to 5%, are significantly reduced. We expect an overall efficiency of better than 97%.

Figure 3: Spot diagram of the F/N adaptations optics



3.2 Collimators

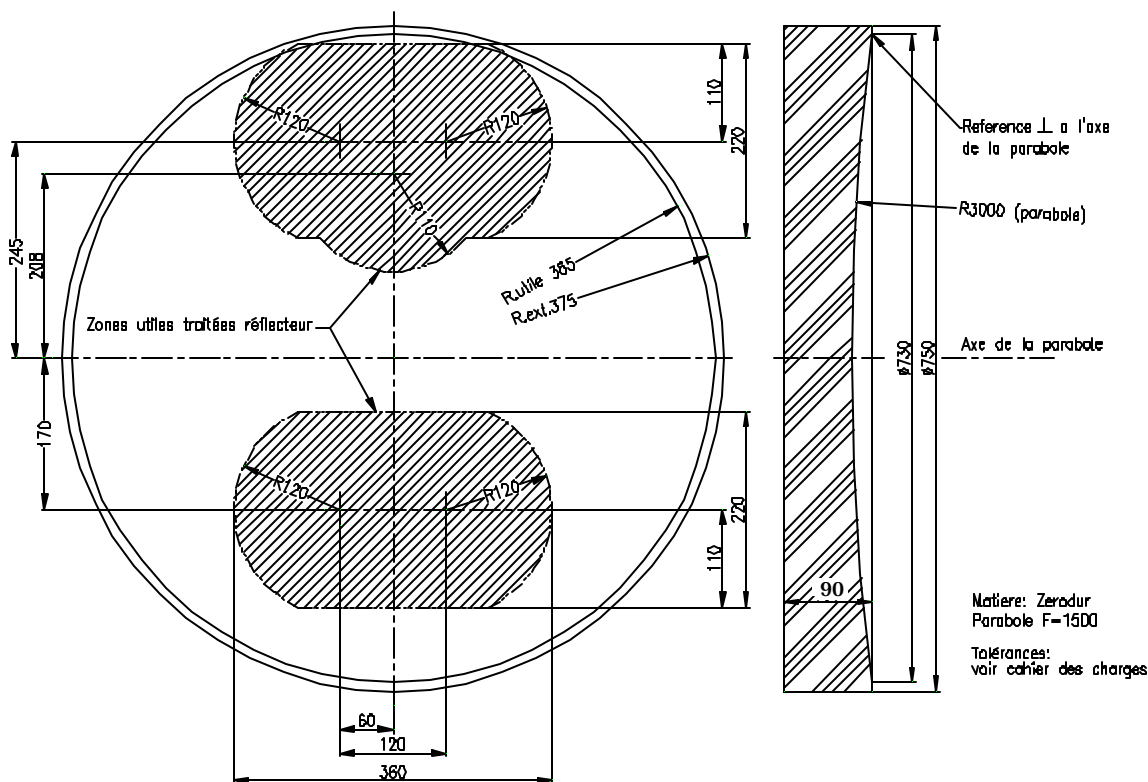
As mentioned above, the collimator, the collector, and the transfer collimator are grouped into one single parabolic mirror. The single mirror solution has been preferred because it reduces the overall costs and increases the mechanical stability. The 750mm \varnothing mirror is made of standard-grade Zerodur®. The surface quality was originally specified over 730 mm but will be guaranteed only over 710 mm. Of the total surface only two sub-areas of the parabola will be

used. The optical performances will be optimized for these areas. Figure 4 shows the parabola with the used areas. The characteristics of the parabola are summarized in Table 2.

Table 2: Characteristics of the collimator parabola

Focal length	1560 mm
Total diameter	750 mm
Clear diameter	730 mm
Thickness at the edge	90 mm
Optical quality in used areas	30 nm RMS @ $I = 632$ nm 150 nm P-V wrt to best parabola
Micro roughness	< 2 nm RMS
Cosmetics	Compliant with MIL 60-40

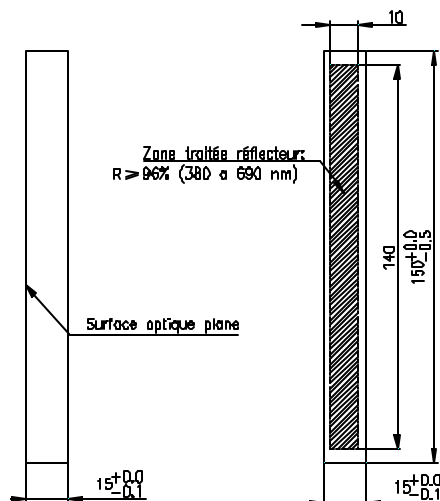
Figure 4: Collimator parabola. The gray zones indicate the used areas.



3.3 Flat Folding Mirror

The flat folding mirror will be located at the position of the intermediate spectrum. The dimensions of the employed mirror are given in Figure 5. The flat mirror is also made of Zerodur® and its optical quality is identical to that of the parabola.

Figure 5: Flat folding mirror



3.4 Echelle Grating

The largest presently available *monolithic* echelle grating has been chosen for HARPS, namely a grating identical to the UVES Red Echelle. The *specified* characteristics are summarized in Table 3 and are detailed in RD-1. The expected performance is somewhat higher. Some of the parameters, as e.g. the groove density, the blaze angle, the efficiency, and the ghost intensity depend mainly on the master grating and will therefore have values similar to those certified in the UVES Red Echelle Test Report (RD-2).

Table 3: Characteristics of the echelle grating

Blank material	Zerodur®, standard grade, monolithic
Dimensions	840 x 214 x 125 mm
Groove density	31.6 gr/mm
Blaze angle	75.07°
Coating	Al
Absolute efficiency (including coating and dead space losses, average of both polarizations, at blaze peak in Littrow, surface average for a 200mm beam)	@380 nm > 60% @450 nm > 64% @550 nm > 64% @680 nm > 63%
Spectral resolution $R=λ/Δλ$ (line FWHM/wavelength)	> 500'000
Spatial resolution (maximal image size in slit direction)	< 4 arcsec
Ghosts intensity (relative to the parent line)	< 0.015%

3.5 Cross-Disperser Grism

3.5.1 General Considerations

In contrast to the preliminary optical design of HARPS a grism has been chosen for cross dispersion instead of a reflection grating. The resulting advantages are:

1. Since the reflecting component in the collimated beam has been replaced by a transmitting element the opto-mechanical stability is increased.
2. The new layout allows us to mount the spectrograph vertically, i.e. with all beams lying in a plane parallel to the gravity. As a result the large echelle grating is mounted edge-on (grooves parallel to gravity) and the main-dispersion direction is horizontal. Both may be considered as an important increase in opto-mechanical stability.
3. The volume of the spectrograph is considerably reduced which is of non-negligible importance for the realization of the vacuum vessel.
4. The risks of ghost images arising from multiple reflection between CCD and reflection grating seems to be reduced in the case of a grism. A comparative study has not been performed, however, since this is not the main driver.

3.5.2 Transmission Efficiency

The optical efficiency for a grism with low groove density is comparable with its equivalent reflection grating. Analysis of measured transmittance curves of existing grisms having similar characteristics have shown that 70% blaze efficiency is easily attained and that 75% to 80% can be expected (references: J. Hoose at Richardson Grating Laboratory, W. Fuertig and W. Seifert at Landessternwarte Heidelberg). These value are very similar to the efficiency values expected for a reflection grating.

Nevertheless we preferred to perform a numerical calculations of the grism efficiency for the chosen parameters, and in a second step, to optimize them for HARPS. Prof. Nevère of the U3 University of Marseille, kindly accepted to perform for us this calculations by means of a numerical code especially developed for transmission gratings and grisms. The results are very encouraging and are presented in Table 4.

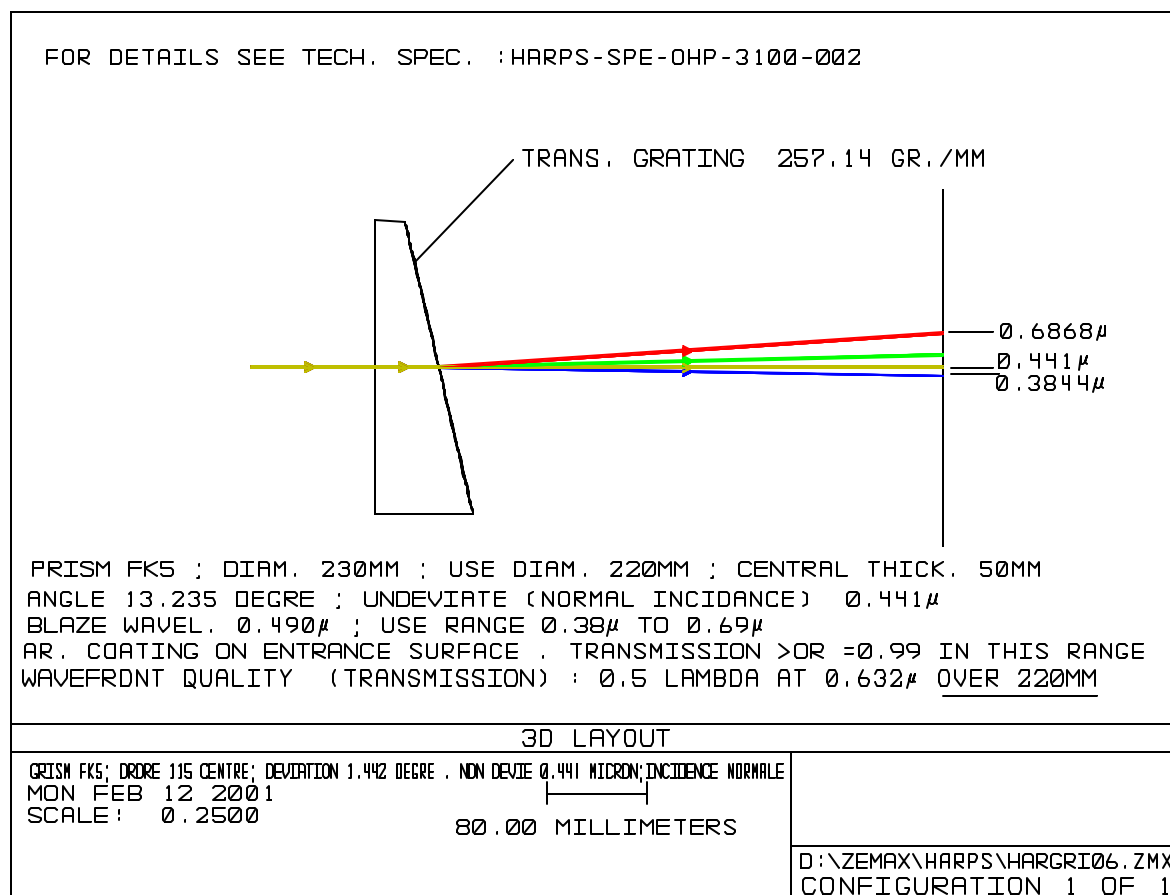
Table 4: Calculated grism efficiency for the parameters shown in Table 5

Wavelength [nm]	Transmission efficiency [%]		
	TE	TM	Unpolarized
380	59	60	59
400	69	69	69
450	82	81	82
480	85	83	84
500	85	83	84
550	82	79	80
600	76	72	74
650	68	65	66
690	63	59	61

3.5.3 Operating Conditions

Figure 6 shows the grism in its operating conditions. The incoming beam is inclined by about 1.43° with respect to the plane defined by the optical bench. The prism apex angle has been chosen to make the outgoing beam axis, and consequently the optical axis of the camera optics, parallel to the collimator axis and to the optical bench.

Figure 6: Operating condition of the cross-disperser grism



3.5.4 Characteristics of the Cross-Disperser Grism

The relevant parameters of the cross-disperser grism of HARPS are given in Table 5. For more details concerning the grism we refer to RD-3.

Table 5: Characteristics of the grism

Prism material	Glass FK5 Schott class NH3/A
Prism dimensions	homogeneity $\Delta n < \pm 2.10^{-6}$ circular $\varnothing 230 \text{ mm} + 0.2 \text{ mm}$ center thickness $50 \text{ mm} \pm 0.2 \text{ mm}$ Apex angle = 13.235°
Grating	257.14 gr/mm $\pm 0.1\%$
Order	1 (or -1)
Minimum ruled area of master grating	$\varnothing 220 \text{ mm}$
Used spectral range	[380 nm – 690 nm]
Blaze wavelength (maximum efficiency of the final grism)	490 nm $\pm 5-15 \text{ nm}$
Resin	"Regular" Bausch & Lomb (TBC) ($n = 1.5981 @ 490 \text{ nm}$)
Groove angle	$\approx 14.5^\circ$ to be optimized for blaze wavelength
Parallelism between the edge of prism and the grooves	$\pm 0,5^\circ$
Wavelength with no deviation	@ 441 nm (λ_{BLAZE} is deviated edge side)
AR Coating of the bare face	Multilayer $T > 98.5\%$ in spectral range average $T > 99\%$
Absolute transmission of the final grism	λ_{nm} 400 500 650 $T >$ 0,60 0,75 0,60
Wavefront quality (transmission)	$\lambda/2$ minimum over $\varnothing 220 \text{ mm}$ at 632 nm
Ghosts and diffuse light	After « the state of the Art »
Operation in vacuum	At least 10 years without degradation

3.6 Camera Optics

3.6.1 Description of the Camera Optics

After having ordered the camera optics, one of the glasses, the Schott PSK3, turned out not to be available. This glass has been replaced now by BK7 and the optimization repeated. The results are still very satisfactory, although the correction of the chromatism is somewhat lower than in the previous solution.

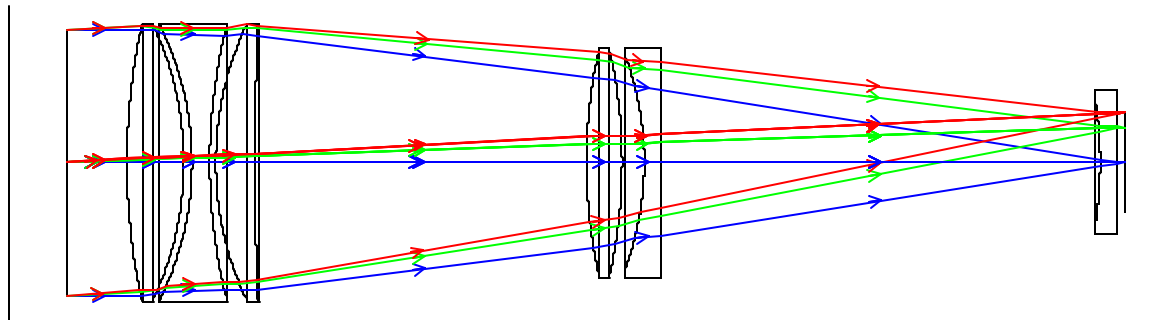
For more details concerning the HARPS camera optics we refer to RD-4. The camera optics is a full dioptric system consisting of 6 lenses. A ray tracing of the camera optics only is shown in Figure 7. The material used are Ohara SFPL53 – Schott BK7 – Ohara SFPL51 for the first triplet, Ohara SFPL51 – Schott BK7 for the doublet, and Synthetic Silica for the field lens which is used also as vacuum window of the detector head. The lens data of the camera optics are given in Table 6. The first triplet is not cemented to avoid risk of breakage due to the large difference of thermal expansion coefficient between its lenses. The additional degrees of freedom allow also

correcting for aberrations. Because of the low number of lenses used and since the A/R coating are very efficient in the covered wavelength region this solution has been preferred against a more expensive cemented solution with its risks.

Table 6: Lens data of the camera optics

Surface	Thickness	Radius	Clear dia.	Total dia.	Glass	Index
OBJ	infinity				AIR	1.00000
STO	50		220		AIR	1.00000
2	48	529.36	220	230	SFPL53	1.44015
3	6.79	-263.34	220	230	AIR	1.00000
4	15	-251.78	220	230	BK7	1.51924
5	5.08	458.3	220	230	AIR	1.00000
6	33	263.34	220	230	SFPL51	1.49886
7	279.85	2419.59	220	230	AIR	1.00000
8	30	420.23	180	190	SFPL51	1.49886
9	18.73	-420.23	180	190	AIR	1.00000
10	15	-251.78	180	190	BK7	1.51924
11	369.823	-4795	180	190	AIR	1.00000
12	15	-322.28	100	120	SILICA	1.46052
13	6	infinity	100	120	AIR	1.00000
IMA		infinity				

Figure 7: Ray tracing of the camera optics



3.6.2 Optical Characteristics

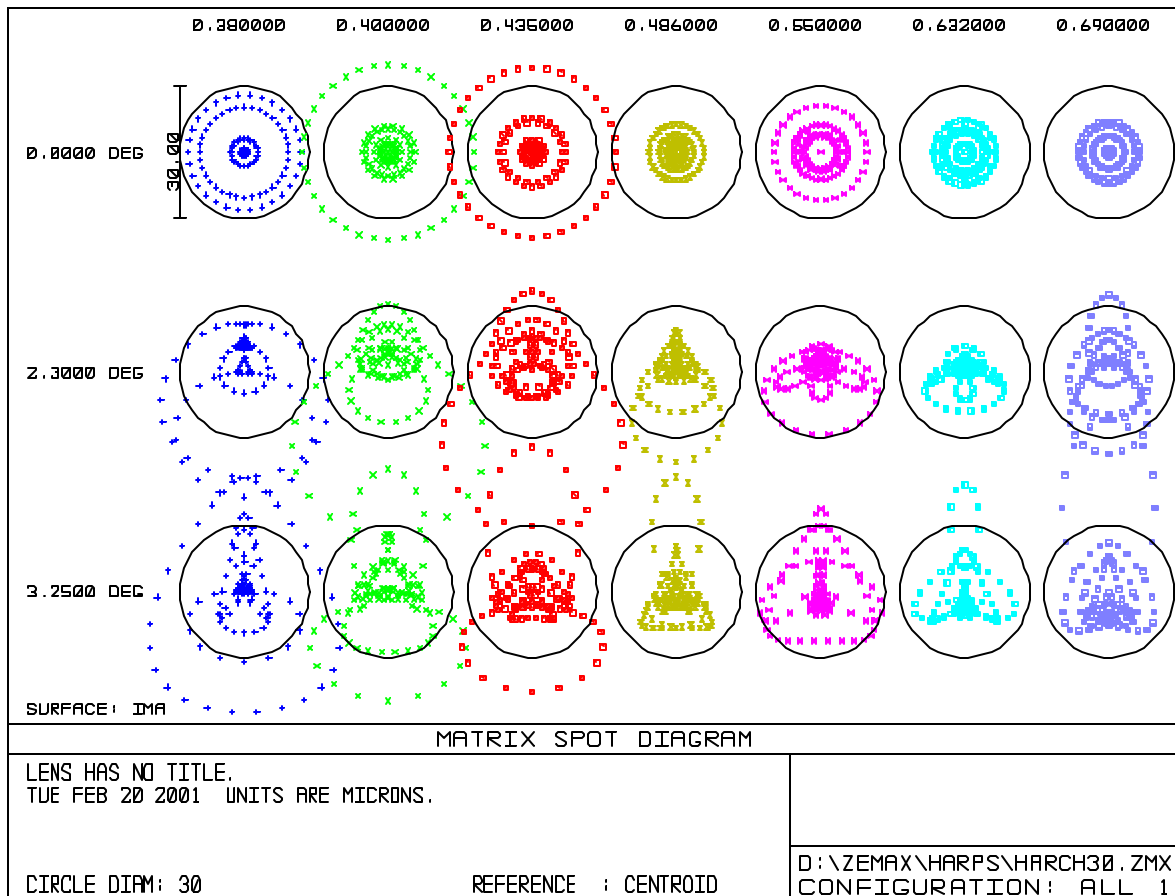
The optical characteristics of the HARPS camera optics are summarized in Table 7.

Figure 8 shows the spot diagrams of the camera optics only. For the spot diagrams of the camera optics the cylindrical surface of the field lens (which corrects the field curvature produced by the parabolic mirror) had to be replaced by a flat surface. In order to perform the tests of the camera optics as stand-alone component this kind of modified field lens will be required. We have therefore included it to the camera optics deliverables.

Table 7: Characteristics of the camera optics

Focal length	725 mm
F/N number	3.3
Spectral range	380 to 690 nm
Central wavelength	531 nm
Object position	At infinity
Entrance pupil	220 mm accepted
Number of lenses	6 (not cemented)
Back-focal length	6 mm
Field dimension (x,y)	Rectangular, 62.74 x 61.44 mm
Chromatism	Both longitudinal and lateral corrected
Field curvature	Corrected either for camera only or full spectrograph

Figure 8: Spot diagrams of the camera optics only



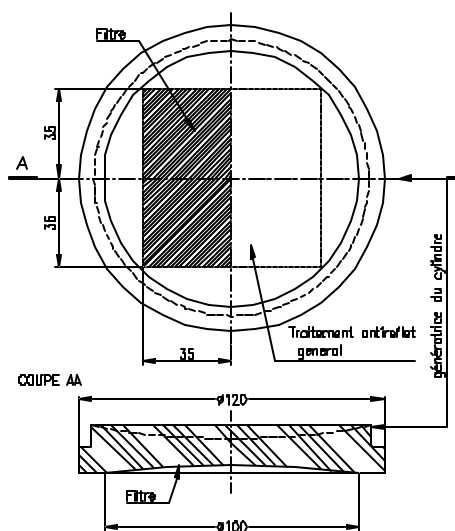
3.6.3 Camera Optics Efficiency

In the HARPS wavelength range very good coatings with an average transmittance $T > 99\%$ are available. The total efficiency, including glass transmittance, is therefore expected to be higher than 85% in average.

3.6.4 Order-Separating Filter

Because of the cross disperser being a grism the red part of the used first order must be separated from the blue part of the unused second order. While wavelengths below 360 nm must be completely rejected, high transmittance is required above 380 nm. A high-pass filter at the entrance of the spectrograph would have to be very steep and it would have poor transmission between 380 nm and 400 nm, yet. Therefore we have preferred to locate a filter on the front surface of the field lens. The filter is coated only on the side of the field lens corresponding to the red part of the spectrum. The layout is shown in Figure 9. The requirements to the filter are, for this solution, much less stringent, and high transmittance is guaranteed. The efficiency will be higher than 95% above 530 nm while light below 400 nm is completely rejected.

Figure 9: Field lens and order-separating filter



Chapter 4: Spectrograph Performances

4.1 Spectral Format

The spectral format is shown in Figure 10. The horizontal axis represents the main-dispersion direction. It is denominated y for consistency with the general lens data. The vertical x axis corresponds to the cross-dispersion direction. The unit is [mm] for both axis. The spectrum ranges from 383 nm at the lower left edge to 690 nm at the upper right edge. The simulation shows the spectra of the object and reference (dashed) fibers. The camera optics F-number has been optimized to match the dimensions of the CCD chip. The bright part of the order indicates the free spectral range. The reference fiber spectrum is displaced by about $260 \mu\text{m}$ which corresponds to half the minimum inter-order distance attained in the blue. Due to the dispersion characteristics of the grism the inter-order distance between the different echelle orders increases from the blue towards the red from a minimum of 34 pixels to a maximum of 100 pixels. The gap between the two 2k4 CCD is situated at $x=0$. The inclination of the orders varies as a function of the order. During optical alignment the CCD will be slightly tilted around the z -axis in order to align the central order with respect to this gap. The gap has been specified to be smaller than 1.3 mm. This way, only one object order, order 115, is lost in the gap between the two CCDs.

Figure 10: Spectral format. The gray rectangles represent a mosaic of two 2k4 CCDs.

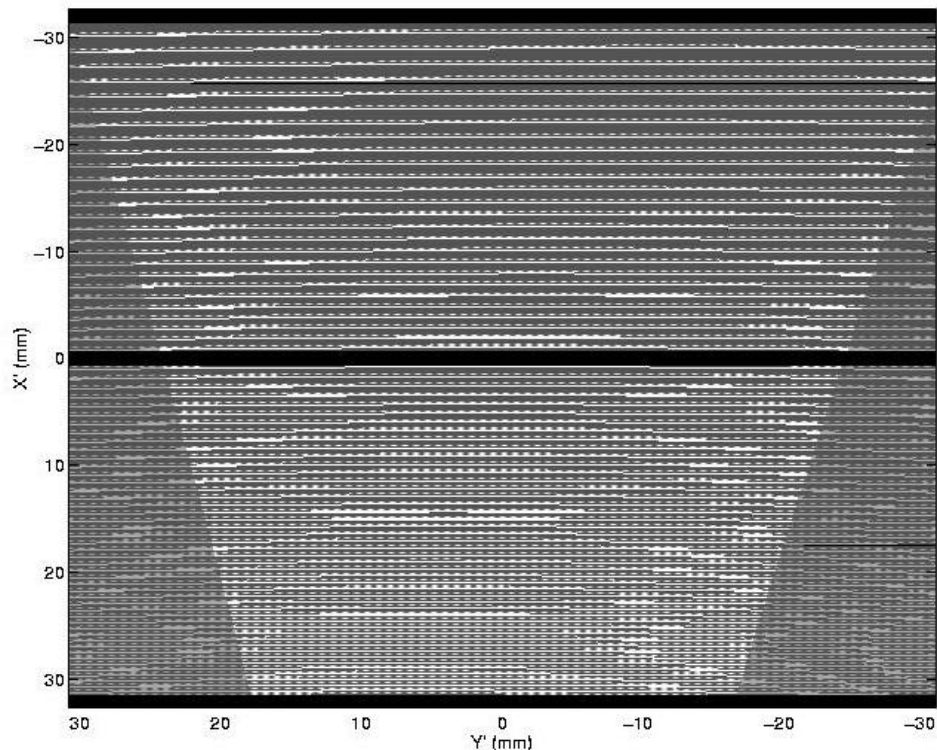


Table 8 indicates the inter-order distance, the inclination with respect to the CCD border, and the “deflection” for the three orders at the top, center, and bottom of the CCD. The deflection is measured as the distance of a point at the center of the order with respect to the straight line which connects the points at the left end of the order to the point at the right end.

Table 8: Geometrical characteristics of the echelle orders

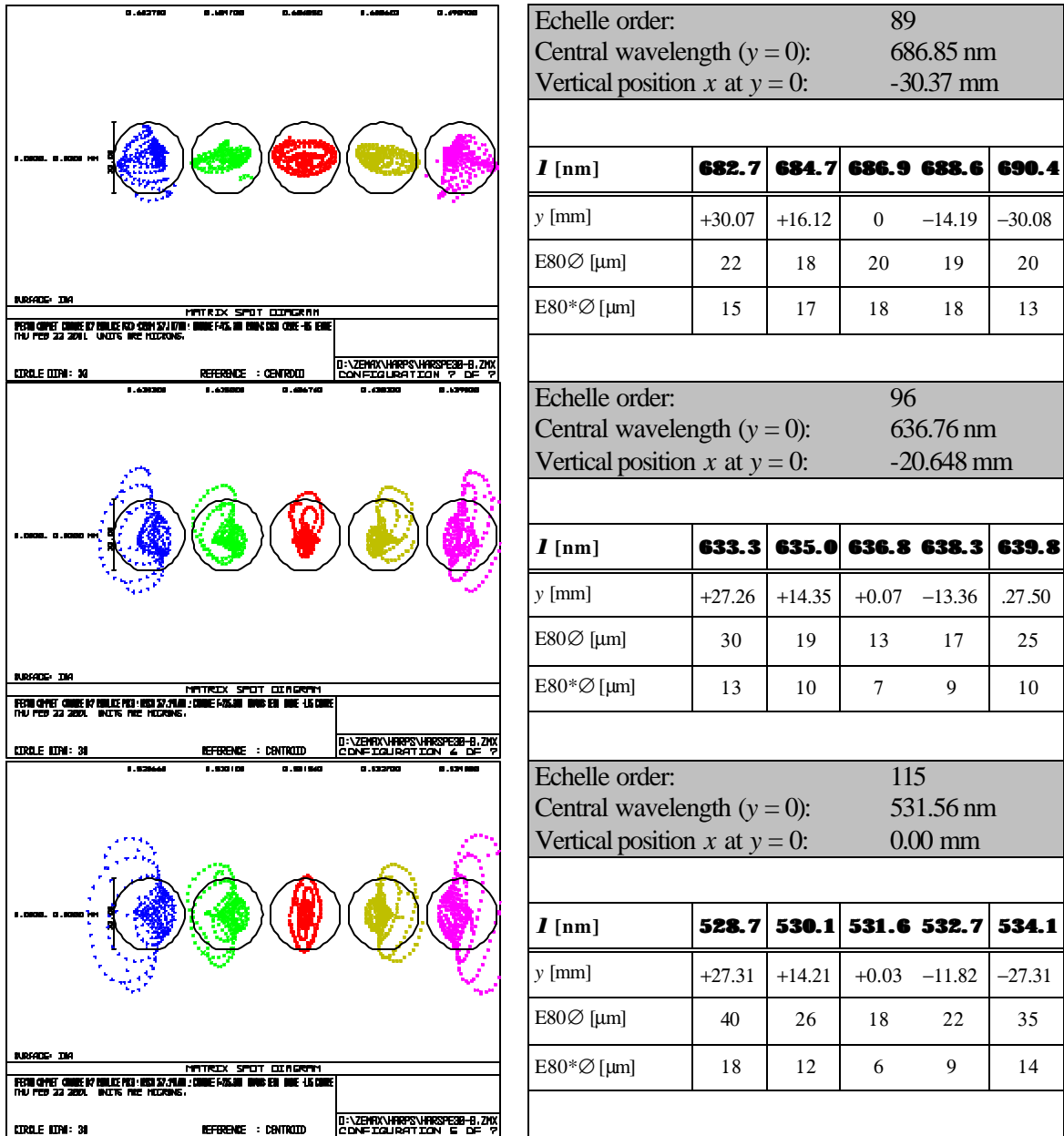
Order N°	Central wavelength [Å]	Total spectral range $\Delta\lambda$ [Å]	Position X at center [mm]	Inter order distance dX [mm]	Slope [deg]	Curvature [mm]
89	6868.5	78.8	-30.371	1.510	1.424	-0.192
90	6792.2	77.9	-28.893	1.478	1.411	-0.197
114	5362.3	61.6	-0.928	0.940	1.139	-0.267
115	5315.6	61.0	-0.003	0.925	1.130	-0.269
116	5269.8	60.5	0.907	0.910	1.122	-0.271
159	3844.6	44.1	30.125	0.523	0.886	-0.352
160	3820.6	43.8	30.643	0.518	0.881	-0.353
161	3796.9	43.6	31.156	0.513	0.876	-0.353

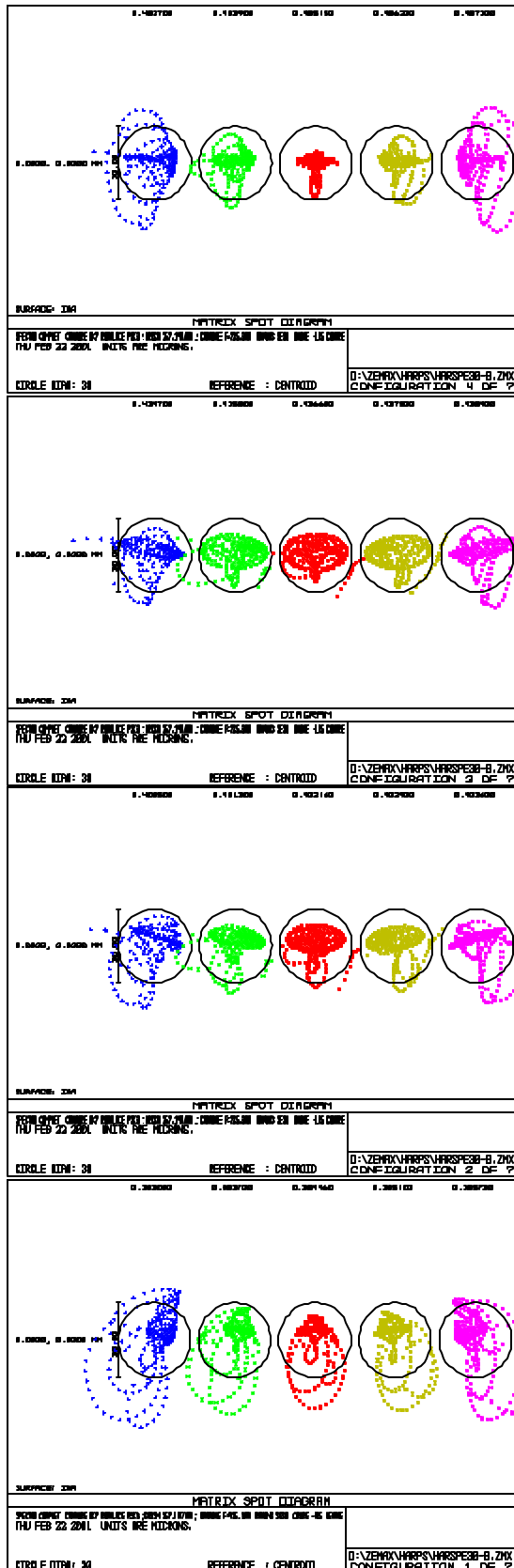
4.2 Spot Diagrams and Image Quality

In Figure 11, on the left side, spot diagrams for 7 echelle orders are shown. Each order has been computed at 5 different wavelengths. The wavelengths taken on each end of the order correspond at least to the free spectral range. The size of the circle indicates $30 \mu\text{m}$.

The tables on the right give detailed information concerning each spot. Besides the wavelength and its corresponding y -position, also the *diameter* of the 80%-encircled energy E80 is shown. E80* indicates the 80%-energy bin in the direction of main dispersion. This parameter rather than E80 is relevant for the spectral resolution. It can be seen that the values never exceed $21 \mu\text{m}$. Since the projection of the fiber exit on the CCD measures $60 \mu\text{m}$, the spectral resolution of the spectrograph is limited by the entrance slit.

Figure 11: Spot diagrams of the HARPS spectrograph





Echelle order:	126				
Central wavelength (y = 0):	485.15 nm				
Vertical position x at y = 0:	+9.27 mm				
I [nm]	482.7	483.9	485.2	486.2	487.3
y [mm]	+25.44	+13.40	+0.07	-11.89	-25.34
E80Ø [µm]	29	18	12	16	24
E80*Ø [µm]	17	14	9	12	13
Echelle order:	140				
Central wavelength (y = 0):	436.60 nm				
Vertical position x at y = 0:	+19.16 mm				
I [nm]	434.7	435.8	436.6	437.5	438.4
y [mm]	+22.50	+10.05	+0.50	-10.85	-22.96
E80Ø [µm]	24	23	22	22	22
E80*Ø [µm]	21	20	20	20	18
Echelle order:	152				
Central wavelength (y = 0):	402.16 nm				
Vertical position x at y = 0:	+26.35 mm				
I [nm]	400.5	401.3	402.2	402.9	403.6
y [mm]	+21.09	+11.25	+0.12	-10.00	-20.13
E80Ø [µm]	24	21	21	21	21
E80*Ø [µm]	19	18	18	18	18
Echelle order:	159				
Central wavelength (y = 0):	384.46 nm				
Vertical position x at y = 0:	-30.37 mm				
I [nm]	383.0	383.7	384.5	385.1	385.7
y [µm]	+19.43	+10.37	+0.05	-9.09	-18.56
E80Ø [µm]	38	25	18	21	32
E80*Ø [µm]	18	14	12	12	14

4.3 Optical Efficiency

4.3.1 Mirror Coating

The specified reflectivity of the mirror coatings is 94% at 380 nm and 96% above 400 nm.

4.3.2 Lens AR Coating

In the specified wavelength range AR coating leading to an average transmittance of better than 99% per surface can be applied.

4.3.3 Overall Efficiency

Table 9 shows the calculated spectrograph efficiency at various wavelengths. The total efficiency does not include the CCD quantum efficiency, slit efficiency, the efficiency of the optical fiber link to the Cassegrain Fiber Adapter of HARPS, nor it takes into account the telescope efficiency. The optical gap between echelle grating submasters is included, however. For the camera optics surface an average value of 88% has been assumed, but it should rather be taken as a minimum value. For the echelle efficiency we have put the specified values in the table. The grism efficiency has been assumed 10% lower than the calculated value. Therefore we expect for both, echelle and grism efficiency, to be lower limits.

Table 9: Spectrograph efficiency

I_{nm}	380	400	480	550	650	690
4 mirrors	0.78	0.85	0.85	0.85	0.85	0.85
Echelle (@ blaze)	0.60	0.62	0.64	0.64	0.63	0.63
Grism	0.54	0.64	0.79	0.75	0.61	0.56
Camera optics (glasses)	0.90	0.94	0.96	0.98	0.98	0.98
Camera optics (surfaces)	0.88	0.88	0.88	0.88	0.88	0.88
Order-separating filters	1	1	1	0.95	0.95	0.95
Total	0.20	0.28	0.36	0.34	0.27	0.25

4.3.4 Vignetting

As mentioned in the introduction the entrance pupil has been changed to 208 mm instead of the initial 200 mm. Table 10 shows the calculated transmittance of the system for three different orders. The wavelengths taken within an order are the same as in the spot diagrams in Section 4.2. In this table also the transmittance averaged over an echelle order is shown.

Since the grism and the camera optics are able to accept a beam of 220 mm we have computed the transmittance also for this pupil diameter. The beam becomes in that case somewhat more vignetted by various components of the spectrograph.

For a 208 mm entrance pupil vignetting is very low and concerns only the very left part of the spectrum. This is due to the anamorphose arising from the echelle grating. The wavelengths deviated towards the “blue” spectral side of each echelle order form a white pupil on the grism which is larger than the entrance pupil. The beam is consequently vignetted by the grism and by the camera optics entrance.

Table 10: Vignetting through the entire spectrograph.

Order no.	<i>I</i> Pupil	#1	#2	#3	#4	#5	Average Transmittance
89	Ø 208	90.4%	97.2%	99.7%	100%	99.9%	97.5%
	Ø 220	81.9%	89.5%	95.6%	97.2%	96.9%	92.0%
115	Ø 208	92.1%	98.1%	100%	100%	100%	98.0%
	Ø 220	84.2%	90.9%	96.3%	97.8%	98.0%	93.5%
159	Ø 208	95.6%	98.5%	99.9%	100%	100%	99.0%
	Ø 220	88.2%	92.5%	95.8%	97.4%	98.2%	94.5%

4.4 Ghost Images and Parasitic Light

4.4.1 Camera Optics Ghost Analysis

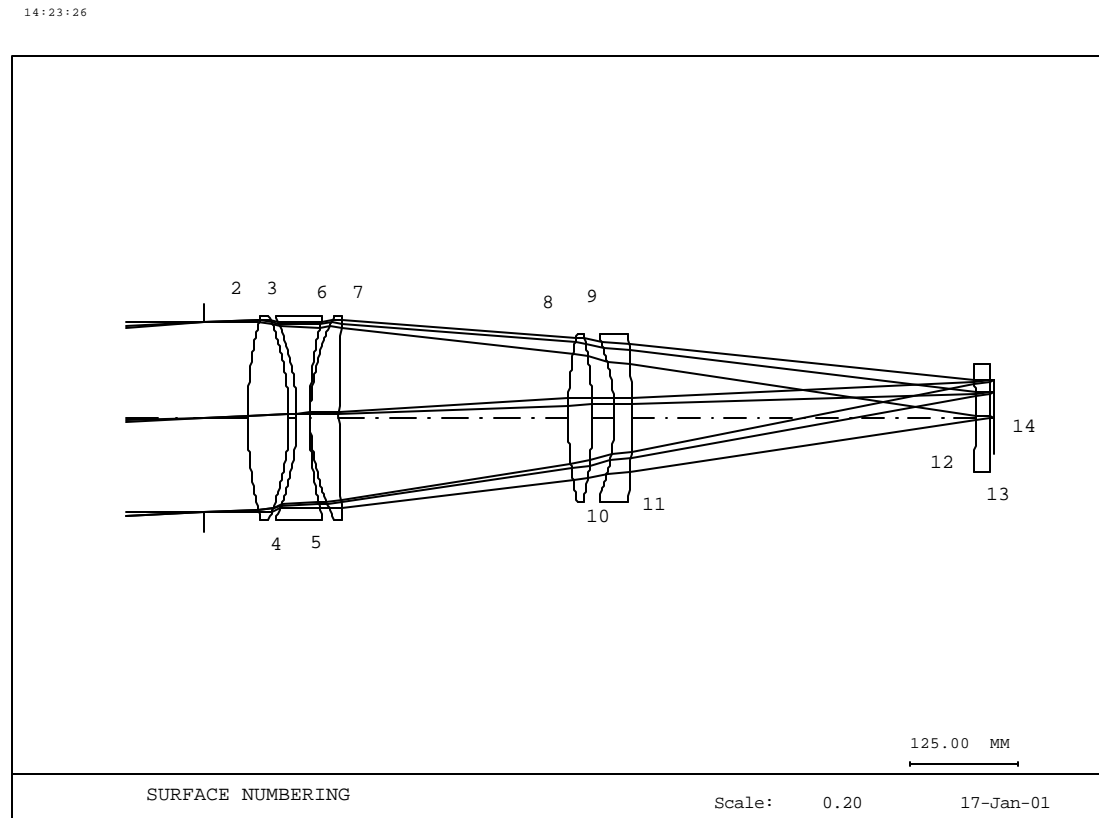
4.4.1.1 Introduction

The ghost analysis has been performed using paraxial rays. The results obtained are most of the time not corresponding to what will really happen because this analysis does not take into account the size of the optical element and most of the ghost images are strongly vignetted. But this method can be used to select (out of 78 possible combinations) the most critical ghosts, which can be separately analyzed with real rays to see if they are really critical.

4.4.1.2 Surface Numbering

Each surface has a number according to Figure 12 which will be used in the analysis.

Figure 12: Numbering of the lens surfaces



4.4.1.3 Table of All Possible Ghosts

The analysis has been limited to 2 reflections.

How to read the table :

REFL1 is the number of the surface on which the light is reflected for the 1st time

REFL2 is the number of the surface on which the light is reflected for the 2nd time

Radius is the radius of the ghost image created by REFL1 and REFL2 on the detector plane

Position is the radial distance on the detector plane of the ghost image created by REFL1 and REFL2 of a object located originally at 42 mm. In other terms position is the radial distance of the chief ray (FOV 42 mm)

Two kinds of ghost images can disturb the observations:

- Bright focused ghost image (value provided by the column radius)
- Sky concentration effect. This sky concentration is in fact a small image of the telescope pupil located near the detector. This effect can be seen from the table of the numbers in the column position and radius are simultaneously small.

REFL 1	REFL 2	Radius	Position	REFL 1	REFL 2	Radius	Position
3	2	-1132.42	-13.61	12	5	422.13	338.32
4	2	-1105.46	-17.81	13	5	390.08	-603.39
5	2	23.60	34.80	14	5	404.81	-613.39
6	2	199.84	43.96	7	6	-717.61	-16.55
7	2	-366.41	3.19	8	6	-794.74	-376.86
8	2	-357.21	-158.87	9	6	655.68	82.91
9	2	189.31	11.20	10	6	978.11	203.55
10	2	328.38	59.80	11	6	-96.71	-209.82
11	2	-86.63	-101.56	12	6	671.65	559.93
12	2	313.66	249.05	13	6	618.99	-934.07
13	2	290.02	-451.15	14	6	641.35	-949.25
14	2	301.09	-458.66	8	7	174.49	120.49
4	3	-82.72	41.50	9	7	-522.45	-111.82
5	3	1447.85	128.62	10	7	-614.25	-158.50
6	3	1779.05	154.43	11	7	-133.77	20.00
7	3	804.70	122.20	12	7	-105.16	-132.34
8	3	1323.72	721.27	13	7	-93.49	92.61
9	3	-2030.39	-370.19	14	7	-94.76	93.47
10	3	-2619.49	-621.17	9	8	-419.10	-103.66
11	3	-223.18	284.85	10	8	-442.36	-126.02
12	3	-1013.80	-955.91	11	8	-171.63	-28.86
13	3	-925.83	1276.95	12	8	46.83	-10.42
14	3	-954.05	1296.10	13	8	46.95	-124.52
5	4	1411.65	123.02	14	8	50.98	-127.25
6	4	1722.08	147.54	10	9	-150.83	-3.36
7	4	812.31	119.06	11	9	192.63	134.47
8	4	1318.30	715.71	12	9	-392.87	-286.71
9	4	-1995.88	-362.19	13	9	-365.19	595.37
10	4	-2581.11	-610.75	14	9	-380.31	605.64
11	4	-211.54	285.49	11	10	265.09	152.31
12	4	-1012.57	-951.35	12	10	-431.52	-298.87
13	4	-924.97	1279.51	13	10	-402.36	673.23
14	4	-953.33	1298.75	14	10	-419.77	685.05
6	5	218.45	52.99	12	11	-139.37	-122.20
7	5	-485.21	1.54	13	11	-127.98	186.61
8	5	-484.26	-218.14	14	11	-132.32	189.55
9	5	284.32	22.02	13	12	-3.18	50.15
10	5	474.39	89.39	14	12	-5.27	51.57
11	5	-106.11	-135.78	14	13	-1.80	43.04

4.4.2 Ghosts from the Grism

Ghost images might arise from reflections between CCD and one of the grism surfaces, i.e. the blank surface or the replicated surface. In that case the ghost images are focused.

4.4.3 Echelle Grating Ghosts

The previously discussed analysis does not consider echelle-grating ghosts which produces diffused light across the CCD and in the space between the echelle orders. Because of the high quality of the echelle grating, which is identical to the UVES red echelle grating, these ghosts seem not to be of importance. From the test results on the UVES red echelle grating (RD-5) it can be seen that the ghost's relative intensity to the parents line never exceeds the value of 8×10^{-5} .

4.4.4 Conclusions

The presented conclusions assume following values:

Incoming intensity:	1
CCD reflectivity:	0.1
Reflectivity of AR-coated surfaces:	0.01
Reflectivity of grism (plain surface):	0.01
Reflectivity of grism (replicated surface):	0.05

The camera optics ghost analysis shows that there is no evidence of disturbing ghost images arising from the camera optics. For example, the smallest ghost image produced has a diameter of 1.8 mm. It represents a reflection between the CCD and the last lens surface. In that case the ghost image is formed very close to its parent. If we assume a strong emission line of $60 \mu\text{m}$ in diameter (image size of the fiber), the relative intensity per pixel of its ghost image is about 10^{-6} , which is even smaller than the read-out noise over CCD dynamic range.

All other ghosts have much larger image sizes and they might only contribute to a very weak and diffused continuum across the whole CCD. If we take the worst case of a reflection between the CCD and a lens surface and if we consider a filling factor of the CCD by the echelle spectrum of about 1/100, the continuum might attain a level of 10^{-5} of the average intensity in the orders. In the blue spectral region, where the optical efficiency of the spectrograph is about 5 times lower than for the red orders, the continuum contribution will attain at maximum 5×10^{-5} , which is still well below the specified 10^{-4} of the local continuum. No effects at all are expected on the RV measurement.

The only important ghosts arise from the reflection between CCD and grism. These ghosts are theoretically focussed and may therefore attain high intensities. However, the efficiency of the replicated surface will be in general very low since the blaze condition is not fulfilled. If we take a very pessimistic case with high grism efficiency of about 40% the reflection between CCD and the blank surface of the grism will produce ghosts with 1.6×10^{-4} relative intensity.

Reflections between the CCD and the replicated surface of the grism could produce even brighter ghosts. Assuming again 40% grism efficiency their relative intensity would attain 2×10^{-3} . If we consider the operation condition of the grism described in Figure 6, however, the blaze condition is never fulfilled for any of the wavelengths, and the grism efficiency of the concerned orders will be much lower. We estimate that the relative efficiency lies in worst case again in the order of few 10^{-4} .

4.5 Environmental Sensitivity

4.5.1 Thermal Influence

4.5.1.1 Structure

The only relevant instrumental drifts could be produced by a varying temperature gradient between the right and the left side of the 700 mm broad optical bench. For a stainless-steel bench ΔX becomes rather important having a value of $\Delta X = 40 \mu\text{m}/\Delta^\circ\text{C}$. However, we do not expect strong temperature variations of the spectrograph. The temperature stability of the surrounding vacuum vessel is specified to $\pm 0.05^\circ\text{C}$. In addition to that argument we have also to consider that the instrument stability will not be sensitive to temperature gradient but to their variation. The thermal study presented in RD-6 shows that, due to the high thermal impedance between vacuum vessel and spectrograph, a given temperature gradient on the vessel is attenuated by a factor of ten. Thus, we do not expect variations of the temperature gradient across the optical bench to be higher than 0.01°C . The corresponding uncorrected RV drift would then be of 20 m/s. The time constant of these variations induced by external perturbations is typically of two days. Short-term variations are consequently expected to be much lower, so that the required 10 m/s short-term stability specified in AD-1 should be attained easily.

These values should in any case be compared to typical drifts of the CORALIE spectrograph, which may produce drifts of several 100 m/s during a night, mainly due to atmospheric pressure variations. CORALIE has demonstrated that these drifts are well compensated by the simultaneous-thorium method used in HARPS.

4.5.1.2 Camera Optics and Grism

The following Table 11 shows the behavior of the grism-camera optics system under a temperature variation of $\Delta T = 1^\circ\text{C}$ at an ambient temperature of 20°C . Again the calculation has been carried out for three different echelle orders indicated by their number. ΔX corresponds to a drift of an echelle order in cross-dispersion direction and ΔY is the dilatation of the order caused by variations of the scale factor. ΔZ represents defocus and is measured in terms of variations of the back-focal distance. *All Value are in $[\mu\text{m}]$.*

Table 11: Stability of HARPS (non compensated)

	D [mm] for $\Delta T = 1^\circ\text{C}$		
	ΔX	ΔY	ΔZ
Order 89	+4.0	+3,5	+75
Order 115	+0,5	+3,5	+73
Order 159	-3,0	+3,5	+82

ΔX and ΔY are relatively small effects but not insignificant. However, concerning the stability, we refer to what has been said in the previous section. ΔZ variations, on the other hand, are clearly the dominant effect. They are acceptable for the specified temperature-control accuracy, but an athermalization of the camera optics is preferred. In any case, effects on focus or scale factor do not influence the RV-measurement at first approximation. The reason is that all effects are

symmetric with regard to the x axis. Thus, a possible drift would affect the left end of an echelle order by exactly the same drift but with opposite sign than its right end.

4.5.1.3 Thermal Compensation

The HARPS camera optics shows relatively important temperature coefficient. Since the Spectrograph is temperature controlled an athermalization of the camera is not "mandatory". However, in view of the high-accuracy RV measurements, a better stability of the camera is suited. The thermal compensation has to perform three tasks:

1. Compensate for focus changes
2. Compensate for scale factor changes
3. Compensate for the movement of the orders perpendicular to the order direction and the change of cross-dispersion power, which are caused by the dilatation of the cross-disperser grism (prism) and by variation dn/dT of the refractive index.

The last point has been solved using a grism based on a FK5 prism. For FK5 the two effects mentioned under point 3 compensate each other to a very satisfactory degree.

For point 1 and 2 following solution has been found: The fifth camera lens (BK7) is moved by about $\Delta Z = 30 \mu\text{m}/^\circ\text{C}$. Movement of this lens corrects for both, focus and scale factor. Mechanically it is realized by means of an invar bar acting on the DURAL lens support.

The following Table 12 shows the behavior of the *compensated* grism-camera system. The conditions are identical to those in Table 11. *All Value are in $[\mu\text{m}]$.*

Table 12: Stability of HARPS (*compensated*)

	D [μm] for $DT = 1^\circ\text{C}$		
	DX	DY	DZ
Order 89	+0,8	-0.2	0
Order 115	+0,5	-0.2	0
Order 159	+0,3	-0.2	0

4.5.2 Effects of Air Pressure

Since the spectrograph will be operated in vacuum we have calculated the change of focus and image quality when passing from 1000 mbar to vacuum. The results are shown below. Again the defocus is measured as the distance between the fifth camera optics lens and the field lens:c

Table 13: Changes in focal length in vacuum

Variation of the focal length	-1,45 mm
Defocus	-0,75 mm
Change in central wavelength	-0,13 nm
Variation of the image quality	Very low, mainly chromatic

If we consider a given wavelength, this wavelength will change slightly its position on the CCD. At the center of the CCD this movement will amount to about 1.3 mm in direction of main dispersion, and 0.015 mm in direction of cross-dispersion. Note however, that the "blaze position" (position of maximum efficiency on an echelle order) remains unchanged. In other words, when passing to vacuum the spectral format will be the same, but to a given CCD pixel will correspond a slightly different wavelength.

Chapter 5: Alignment and Tolerances

5.1 Basic Opto-Mechanical Principles

The mechanical support defines the position of the optical component which is as near as possible to its theoretical position. Adjustment mechanisms are avoided unless they are identified as indispensable. Special attention is paid to this point during the preliminary design of the spectrograph mechanics.

5.2 Main Alignment Controls

The main controls to be carried out during the alignment procedure are:

- Infinity adjustment of the collimator
- Parallelism between the optical axis of collimator, the camera optics, and the optical bench
- Intersection position of the optical axis on different components (collimator, echelle grating, grism)

5.3 Alignment Tools

The preliminary list of alignment tools is:

- HeNe laser to define the optical axis of the collimator
- Mask which reproduces the area of impact of the optical beam on the parabola
- 200 mm \varnothing collimator + auto-collimation microscope for the exact determination of the focusing of the fiber inputs
- 200 mm \varnothing flat mirror (including pre-adjusted support) for replacement of the echelle grating
- 200 mm \varnothing flat mirror (including pre-adjusted support) for replacement of the grism and for overall auto-collimation tests

5.4 Alignment Tolerances

The alignment tolerances of the some important parameter are:

Parameter to be adjusted	Error	Effects on spot diameter
Infinity adjustment of collimator	5 mm	+ 20 μ tilt of the focal plane: 0,3°
Tilt of the flat folding mirror around the axis perpendicular to the spectrograph's symmetry plane	0,1°	+ 5 μ
Tilt of the echelle grating around the axis perpendicular to the spectrograph's symmetry plane	0,1°	No significant effects

Chapter 6: Compliance Matrix

In the following table the Compliance Matrix is presented. It refers to the Verification Matrix presented in AD-1 for Preliminary Design Report. The following terms are employed:

A	Applicable
NA	Non applicable
C	Compliant
PC	Partly compliant (shall be commented)
NC	Non compliant (shall be commented)
NV	Not verified at this stage

The columns in the table refer to:

Section	Section number of AD-1
Title	Section title of AD-1
Item	Referred item
Appl.	Status of applicability
Compl.	Status of compliance
Comments	Comments/Exceptions

Section	Title	Item	Appl.	Compl.	Comments
2.3.3	Spectrograph	1. Operational conditions	A	NV	
		2. Optical parameters	A	C	
		3. Efficiency of the spectrograph	A	C	
		4. Stability	A	C	
		5. Stray light and ghosts	A	PC	Grism local ghosts > 10 ⁻⁴
		6. Exposimeter	A	NV	
		7. Optical alignment	A	NV	

Chapter 7: Appendix

7.1 Spectrograph Lens Data

System/Prescription Data

File : D:\ZEMAX\harps\harspe30-b.zmx
 Title: spectro complet chambre bk7 remplace psk3 ;grism 257.14t/mm ; chambre f=725.3mm
 rayons seso ordre -115 centre
 Date : TUE FEB 20 2001
 Configuration 1 of 7

LENS NOTES:

SURFACE DATA SUMMARY:

Surf	Type	Radius	Thickness	Glass	Diameter	Conic
OBJ	TILTSURF	-	1566.967		0	-
1	COORDBRK	-	0		-	-
STO	STANDARD	Infinity	0		220	0
3	COORDBRK	-	0		-	-
4	STANDARD	Infinity	6.9667		471.4753	0
5	STANDARD	-3120	-1560	MIRROR	710	-1
6	COORDBRK	-	0		-	-
7	COORDBRK	-	0		-	-
8	DGRATING	Infinity	0	MIRROR	849.0344	0
9	COORDBRK	-	1560		-	-
10	COORDBRK	-	0		-	-
11	STANDARD	-3120	-1560.65	MIRROR	710	-1
12	STANDARD	Infinity	1560.65	MIRROR	160	0
13	STANDARD	-3120	-1526	MIRROR	710	-1
14	COORDBRK	-	0		-	-
15	STANDARD	Infinity	-50	FK5	230	0
16	COORDBRK	-	0		-	-
17	DGRATING	Infinity	0		230	0
18	COORDBRK	-	-50		-	-
19	STANDARD	-529.36	-48	S-FPL53	230	0
20	STANDARD	263.34	-6.79		230	0
21	STANDARD	251.78	-15	BK7	230	0
22	STANDARD	-458.3	-5.08		230	0
23	STANDARD	-263.34	-33	S-FPL51	230	0
24	STANDARD	-2419.59	-279.85		230	0
25	STANDARD	-420.23	-30	S-FPL51	190	0
26	STANDARD	420.23	-18.73		190	0
27	STANDARD	251.78	-15	BK7	180	0
28	STANDARD	4795	-369.823		190	0
29	STANDARD	322.28	-15	SILICA	100	0
30	TOROIDAL	280	-5.95		120	0
IMA	TILTSURF	-			200	-

SURFACE DATA DETAIL:

Surface OBJ	:	TILTSURF	Order	:	Decenter then tilt
X Tangent	:	0	Scattering	:	None
Y Tangent	:	0	Surface 11	:	STANDARD
Scattering	:	None	Aperture	:	Circular Aperture
Surface 1	:	COORDBRK	Minimum Radius	:	0
Decenter X	:	0	Maximum Radius	:	355
Decenter Y	:	0	Scattering	:	None
Tilt About X	:	0	Surface 12	:	STANDARD
Tilt About Y	:	7.646	Aperture	:	Rectangular Aperture
Tilt About Z	:	0	X Half Width	:	7.5
Order	:	Decenter then tilt	Y Half Width	:	75
Scattering	:	None	X- Decenter	:	-40
Surface STO	:	STANDARD	Scattering	:	None
Scattering	:	None	Surface 13	:	STANDARD
Surface 3	:	COORDBRK	Scattering	:	None
Decenter X	:	208.5	Surface 14	:	COORDBRK
Decenter Y	:	0	Decenter X	:	206.75
Tilt About X	:	0	Decenter Y	:	0
Tilt About Y	:	0	Tilt About X	:	0
Tilt About Z	:	0	Tilt About Y	:	-1.442
Order	:	Decenter then tilt	Tilt About Z	:	90
Scattering	:	None	Order	:	Decenter then tilt
Surface 4	:	STANDARD	Scattering	:	None
Scattering	:	None	Surface 15	:	STANDARD
Surface 5	:	STANDARD	Scattering	:	None
Scattering	:	None	Surface 16	:	COORDBRK
Surface 6	:	COORDBRK	Decenter X	:	0
Decenter X	:	-208.5	Decenter Y	:	0
Decenter Y	:	0	Tilt About X	:	13.235
Tilt About X	:	0	Tilt About Y	:	0
Tilt About Y	:	0	Tilt About Z	:	0
Tilt About Z	:	0	Order	:	Decenter then tilt
Order	:	Decenter then tilt	Scattering	:	None
Scattering	:	None	Surface 17	:	DGRATING
Surface 7	:	COORDBRK	Lines / Micron	:	0.25714
Decenter X	:	0	Diffraction Order	:	1
Decenter Y	:	0	Aperture	:	Elliptical Aperture
Tilt About X	:	-75	X Half Width	:	115
Tilt About Y	:	-0.72115	Y Half Width	:	117.987
Tilt About Z	:	0	Scattering	:	None
Order	:	Tilt then decenter	Surface 18	:	COORDBRK
Scattering	:	None	Decenter X	:	0
Surface 8	:	DGRATING	Decenter Y	:	0
Lines / Micron	:	0.0316	Tilt About X	:	-11.793
Diffraction Order	:	-159	Tilt About Y	:	0
Aperture	:	Rectangular Aperture	Tilt About Z	:	-90
X Half Width	:	105	Order	:	Decenter then tilt
Y Half Width	:	418	Scattering	:	None
Scattering	:	None	Surface 19	:	STANDARD
Surface 9	:	COORDBRK	Scattering	:	None
Decenter X	:	0	Surface 20	:	STANDARD
Decenter Y	:	0	Scattering	:	None
Tilt About X	:	75	Surface 21	:	STANDARD
Tilt About Y	:	0.72115	Scattering	:	None
Tilt About Z	:	0	Surface 22	:	STANDARD
Order	:	Decenter then tilt	Scattering	:	None
Scattering	:	None	Surface 23	:	STANDARD
Surface 10	:	COORDBRK	Scattering	:	None
Decenter X	:	208.5	Surface 24	:	STANDARD
Decenter Y	:	0	Scattering	:	None
Tilt About X	:	0	Surface 25	:	STANDARD
Tilt About Y	:	0	Scattering	:	None
Tilt About Z	:	0	Surface 26	:	STANDARD
			Scattering	:	None
			Surface 27	:	STANDARD

```

Scattering      : None
Surface 28      : STANDARD
Scattering      : None
Surface 29      : STANDARD
Scattering      : None
Surface 30      : TOROIDAL
Rad of rev.     :          0
Coeff on y^2    :          0
Coeff on y^4    :          0
Coeff on y^6    :          0
Coeff on y^8    :          0
Coeff on y^10   :          0
Coeff on y^12   :          0
Coeff on y^14   :          0
Scattering      : None
Surface IMA     : TILTSURF
X Tangent       :          0
Y Tangent       :          0
Aperture        : Rectangular Aperture
X Half Width    :          32
Y Half Width    :          32
Scattering      : None

COATING DEFINITIONS:

MULTI-CONFIGURATION DATA:

Configuration 1:

  1 Wavelength 1 :          0.383
  2 Wavelength 2 :          0.3837
  3 Wavelength 3 :          0.38446
  4 Wavelength 4 :          0.3851
  5 Wavelength 5 :          0.38573
  6 Param 2     8 :          -159

Configuration 2:

  1 Wavelength 1 :          0.4005
  2 Wavelength 2 :          0.4013
  3 Wavelength 3 :          0.40216
  4 Wavelength 4 :          0.4029
  5 Wavelength 5 :          0.4036
  6 Param 2     8 :          -152

Configuration 3:

  1 Wavelength 1 :          0.4347
  2 Wavelength 2 :          0.4358
  3 Wavelength 3 :          0.4366
  4 Wavelength 4 :          0.4375
  5 Wavelength 5 :          0.4384
  6 Param 2     8 :          -140

Configuration 4:

  1 Wavelength 1 :          0.4827
  2 Wavelength 2 :          0.4839
  3 Wavelength 3 :          0.48515
  4 Wavelength 4 :          0.4862
  5 Wavelength 5 :          0.4873
  6 Param 2     8 :          -126

Configuration 5:

  1 Wavelength 1 :          0.52866
  2 Wavelength 2 :          0.5301
  3 Wavelength 3 :          0.53156
  4 Wavelength 4 :          0.5327
  5 Wavelength 5 :          0.53408
  6 Param 2     8 :          -115

Configuration 6:

  1 Wavelength 1 :          0.6333
  2 Wavelength 2 :          0.635
  3 Wavelength 3 :          0.63676
  4 Wavelength 4 :          0.6383
  5 Wavelength 5 :          0.6398
  6 Param 2     8 :          -96

Configuration 7:

  1 Wavelength 1 :          0.6827
  2 Wavelength 2 :          0.6847
  3 Wavelength 3 :          0.68685
  4 Wavelength 4 :          0.6886
  5 Wavelength 5 :          0.6904
  6 Param 2     8 :          -89

```

7.2 F/N-Conversion Optics Lens Data

System/Prescription Data

File : D:\ZEMAX\harps\harfibspel0.zmx
 Title: Optique de sortie de fibre f/4 f/7.5
 Date : TUE FEB 20 2001

LENS NOTES:

Fibre diam.=70mu NO air 4.0 ; NO sort. 7.5
 Doublet (S-FPL53+LLF6)+doublet collé sur la férule de la double fibre
 plus court que ceux du scrambler . coma corrigee.

GENERAL LENS DATA:

Surfaces : 8
 Stop : 4
 System Aperture : Object Space NA = 0.124
 Glass Catalogs : schott OHARA MISC SCHOTT_2000
 Ray Aiming : Off
 Apodization : Uniform, factor = 0.00000E+000
 Effective Focal Length : 365.0408 (in air)
 Effective Focal Length : 365.0408 (in image space)
 Back Focal Length : -669.522
 Total Track : 57.21818
 Image Space F/# : 11.04006
 Paraxial Working F/# : 7.541858
 Working F/# : 7.579726
 Image Space NA : 0.06615144
 Object Space NA : 0.124
 Stop Radius : 1.06848
 Paraxial Image Height : 0.2626681
 Paraxial Magnification : -1.876201
 Entrance Pupil Diameter : 33.0651
 Entrance Pupil Position : 209.4092
 Exit Pupil Diameter : 195.7831
 Exit Pupil Position : 1476.626
 Field Type : Object height in Millimeters
 Maximum Field : 0.14
 Primary Wave : 0.536
 Lens Units : Millimeters
 Angular Magnification : -0.2660857

Fields : 3

Field Type: Object height in Millimeters

#	X-Value	Y-Value	Weight
1	0.000000	0.000000	1.000000
2	0.000000	0.140000	20.000000
3	0.000000	-0.140000	20.000000

Vignetting Factors

#	VDX	VDY	VCX	VCY
1	0.000000	0.000000	0.000000	0.000000
2	0.000000	0.000000	0.000000	0.000000
3	0.000000	0.000000	0.000000	0.000000

Wavelengths : 5

Units: Microns

#	Value	Weight
1	0.380000	1.000000
2	0.420000	1.000000
3	0.470000	1.000000

4	0.536000	1.000000
5	0.680000	1.000000

SURFACE DATA SUMMARY:

Surf	Type	Radius	Thickness	Glass	Diameter	Conic
OBJ	STANDARD	Infinity	0	N-BAK1	0.28	0
1	STANDARD	Infinity	9.779237	N-BAK1	3.18	0
2	STANDARD	2.5	2.5	S-FPL51	3.18	0
3	STANDARD	-3.573724	8.5		3.18	0
STO	STANDARD	Infinity	8.625		2.140325	0
5	STANDARD	16.57368	6.081432	S-FPL53	5	0
6	STANDARD	-4	6.421488	LLF6	5	0
7	STANDARD	-8.191333	15.31102		5	0
IMA	STANDARD	Infinity			0.5299045	0